



ELECTRICAL RESISTIVITY STUDIES OF ZR-MG DOPED CHROMIUM SPINEL FERRITES

N. N. SARKAR¹, K. G. REWATKAR¹, V.M NANOTT², C.S PRAKASH³

¹Department of Physics, Dr. Ambedkar College, Deeksha Bhoomi, Nagpur 440010, India

²Department of Physics, Priyadarshini Institute of Engineering and Technology, Nagpur 440019, India

³Department of Physics, S.J.C.Institute of Technology, Chickballapur-562101, Karnataka, India

E-mail: ns.rathinonly4u@gmail.com

ABSTRACT

Nano-sized Zr-Mg doped chromium spinel ferrites with nominal composition, $Mg_{(1+x)}Zr_x(CrFe)_{1-x}O_4$ ($x = 0.2, 0.4, 0.6, 0.8$) were synthesized using sol-gel auto combustion. The structural study of the synthesized iron oxide samples were carried out by X-ray diffraction (XRD). The XRD analysis confirmed face centered cubic structure for all the compositions of $Mg_{(1+x)}Zr_x(CrFe)_{1-x}O_4$ nano-crystallites. The variation in lattice parameter as determined by XRD data agreed with variation of ionic radii of cations. The electrical resistivity (ρ) was calculated across the temperature and was found to decrease with an increase in temperature confirming the semiconducting nature of the synthesized samples. The corresponding activation energies for conduction have been carried out from the plot of log conductivity against $1000/T$ for all of the samples, which display two slopes of separate regions. It was found that the activation energy was higher in the paramagnetic region than in the ferromagnetic region. With an increase in Zr - Mg composition, the electrical resistivity was found to decrease

Keywords: Spinel ferrite, Sol-gel auto combustion, XRD, D.C electrical resistivity, Activation energy.

I. INTRODUCTION

Nano sizes spinel ferrite, having chemical composition $Mg_{(1+x)}Zr_x(CrFe)_{1-x}O_4$ ($x = 0.2, 0.4, 0.6, 0.8$) have cubic system with a unit cell containing eight formula units [1]. In the present system of spinel ferrite there are two types of lattice sites for distribution cation namely A and B sites having tetrahedral and octahedral coordinations, respectively [2]. Generally, the M^{2+} and Fe^{3+} cations are distributed at both the sites normally the Me^{2+} at tetrahedral site and Fe^{3+} at octahedral site. [3]. The variation of cation distribution over the A and B sites leads to different magnetic, electric properties etc. Ferrites are well known of semiconductors by nature at higher temperature, nano-ferrites contain more than 40-50% iron have the most useful materials for applications in telecommunication and high frequency devices. Ferrites have general properties like low dielectric losses, high electrical resistivity, high permeability, thermal stability and are semiconductor in nature. The conduction mechanism of ferrites describe by electrical resistivity of respective material [4]. In case of ferrite the exchange of electrons can be explain with the help of hopping mechanisms between elements having more than one valence state in the equivalent sites of the crystalline lattice.

The method of preparation and substitutions of different composition in the spinel ferrite system can be controlled the electrical properties of ferrite, the higher resistivity of ferrites material is useful for high-frequency and small loss applications.. The substitution of non magnetic ions such as Zr^{4+} - Mg^{2+} in chromium spinel ferrites has strongly affected on their electric-magnetic properties have been reported by El Hiti [6]. In the present research module we studied the change in electrical properties by the substitution of zirconium in Magnesium chromium ferrite. Cr^{3+} ions have strong preference for the octahedral (B) site while Mg^{2+} ions have preference for both tetrahedral and octahedral sites. With a view to understand the conduction mechanism in the mixed Zr-Mg-Cr nano-ferrite system, we have undertaken the study of electrical resistivity as a function of composition and temperature



II. EXPERIMENTAL

2.1 Materials

The raw materials used for sol-gel auto combustion synthesis of $Mg_{(1+x)}Zr_x(CrFe)_{1-x}O_4$ ($x = 0.2, 0.4, 0.6, 0.8$) nanoparticles were magnesium nitrate ($Mg(NO_3)_2 \cdot 6H_2O$), zirconium nitrate ($ZrO(NO_3)_2$), ferric nitrate ($Fe(NO_3)_3 \cdot 9H_2O$), aluminum nitrate ($Cr(NO_3)_3 \cdot 9H_2O$), Urea ($NH_2-CO-NH_2$). All the reagents used for the synthesis of cobalt ferrite nanoparticles were analytical grade.

2.2 Synthesis

$Mg_{(1+x)}Zr_x(CrFe)_{1-x}O_4$ ($x = 0.2, 0.4, 0.6, 0.8$) nanoparticles were synthesized by sol-gel auto combustion method using urea as a fuel. The stoichiometric proportions of metal nitrates to fuel (urea) ratio was taken into separate borosil glass beakers. These were stirred for 15-20 minutes to dissolve completely into distilled water. After complete dissolution they were mixed together. Then the solution was constantly magnetically stirred and heated at 80-90 °C for 6 h on a hot plate. On the formation of viscous gel, then the gel were kept in microwave oven for instant fire at 600 watt. The dried gel started and finally powder was obtained. The as prepared ferrite powder was grinded for 4 hrs and annealed at 800 °C for 4 hrs in muffle furnace.

2.3. Characterizations

In the present work, zirconium and magnesium substituted chromium ferrite samples were synthesized by sol-gel auto combustion method and characterized by X-ray diffraction technique and impedance analyzer. X-ray diffraction patterns of all the samples were recorded in the 2θ range 20° to 80° with scanning rate of 2° per minute using Cu-K α radiation of wavelength 1.5406 Å. The effect of substitution on the electrical properties like resistivity and conductivity etc. was studied using a Impedance analyzer. [5] proposed a principle in which another NN yield input control law was created for an under incited quad rotor UAV which uses the regular limitations of the under incited framework to create virtual control contributions to ensure the UAV tracks a craved direction. Utilizing the versatile back venturing method, every one of the six DOF are effectively followed utilizing just four control inputs while within the sight of un demonstrated flow and limited unsettling influences. Elements and speed vectors were thought to be inaccessible, along these lines a NN eyewitness was intended to recoup the limitless states. At that point, a novel NN virtual control structure which permitted the craved translational speeds to be controlled utilizing the pitch and the move of the UAV. At long last, a NN was used in the figuring of the real control inputs for the UAV dynamic framework. Utilizing Lyapunov systems, it was demonstrated that the estimation blunders of each NN, the spectator, Virtual controller, and the position, introduction, and speed following mistakes were all SGUUB while unwinding the partition Principle.

III. RESULTS AND DISCUSSION

3.1. XRD (x-ray diffraction)

The x-ray diffraction pattern of the sintered Zr-Mg substituted chromium ferrite samples as shown in figure 1, from the (hkl) planes we confirming the cubic spinel structure[7]. The other peaks in the XRD pattern gives evidence for the existence of an extra phase of ZrO_2 [8]. It has been observed from the x-ray diffraction pattern, as the value of "x" increases from $x=0.2$ to $x=0.8$ the intensity peaks of ZrO_2 increases. This may be due to the effect of increase in concentration of Zr^{4+} ions in the samples [9].

The lattice parameter and their respective crystalline size were mentioned in table 1. We notice that the lattice parameter increase gradually with substitution of Zr ions, this may be due to large ionic radius of Zr (0.72 Å) as compare to Fe (0.64Å). Zr^{+4} ions are known to occupy tetrahedral (A) sites due to their strong preference for tetrahedral coordination [10] and Fe^{+3} ions do not have the sufficient occupancy in the cubic system of tetrahedral (A) site. Similarly Cr^{3+} has its occupancy in the octahedral (B) site as discussed earlier.

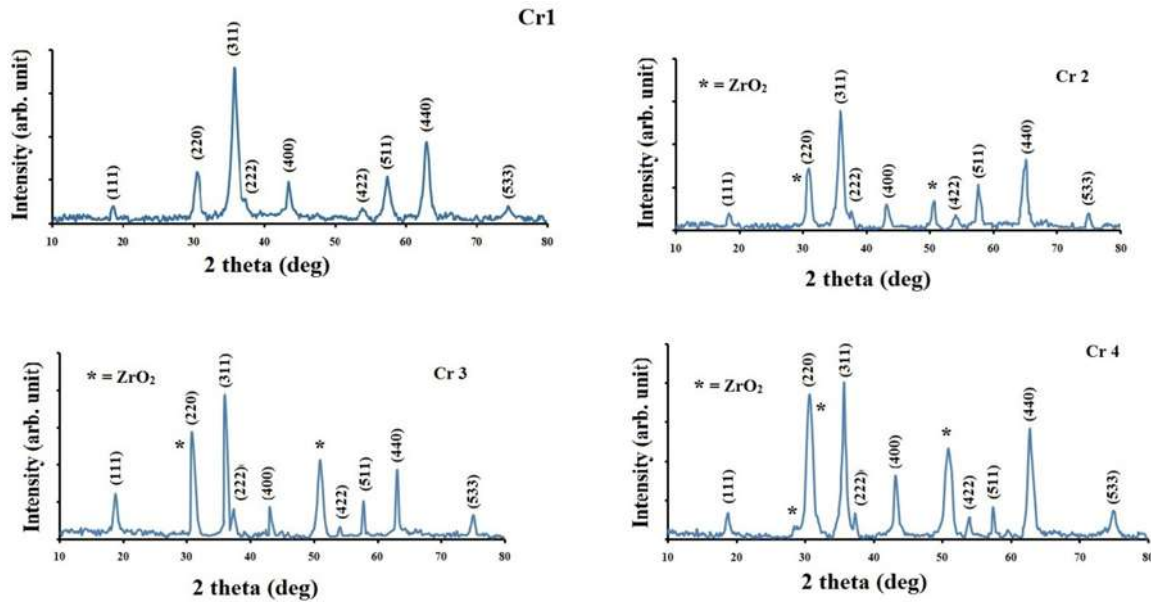


Figure 1. XRD pattern of of $Mg_{(1+x)}Zr_x(CrFe)_{1-x}O_4(x = 0.2, 0.4, 0.6, 0.8)$

Table 1 Lattice parameter

Sr No	Name of compound	symbol	Lattice parameter (Å)	Crystallite size (nm)
1	$Mg_{1.2}Zr_{0.2}(Fe\ Cr)_{0.8}O_4$	Cr1	8.2843	11.392
2	$Mg_{1.4}Zr_{0.4}(Fe\ Cr)_{0.6}O_4$	Cr2	8.3190	11.15
3	$Mg_{1.6}Zr_{0.6}(Fe\ Cr)_{0.4}O_4$	Cr3	8.3321	12.056
4	$Mg_{1.8}Zr_{0.8}(Fe\ Cr)_{0.2}O_4$	Cr4	8.3502	10.62

3.2. Effect of temperature on D.C. Electrical Resistivity

Figure 2 shows that the variation of D.C. electrical resistivity has been observed for all the samples with respective temperature. It is clear from figure 2 that, resistivity goes down with increasing temperature. This fact reveals the semiconducting nature of the prepared ferrites. This could be account to the increase in the drift mobility of electric charge carriers which are activated at higher temperature as shown in figure 3.

The resistivity of all the samples of Zr- Mg-Cr nano-ferrite system at room temperature was tabulated in table 2, it is noticed from table 2 that the resistivity, drift mobility and activation energy all are gradually increases with substitution of Zr and Mg in the chromium spinel ferrite system.



Sample code	Resistivity (ρ) Room temp. $\times 10^6$ M Ω -cm	Drift mobility (μ_d) at 550k $\times 10^{-8}$ (M 2 /v-s)	Activation Energy E_p (eV)	Activation energy E_r (eV)	ΔE (eV)
Cr 1	3.37	3520	0.643	0.604	0.039
Cr 2	4.74	1760	0.659	0.659	0.042
Cr 3	6.00	724	0.678	0.630	0.048
Cr 4	7.71	455	0.703	0.650	0.053

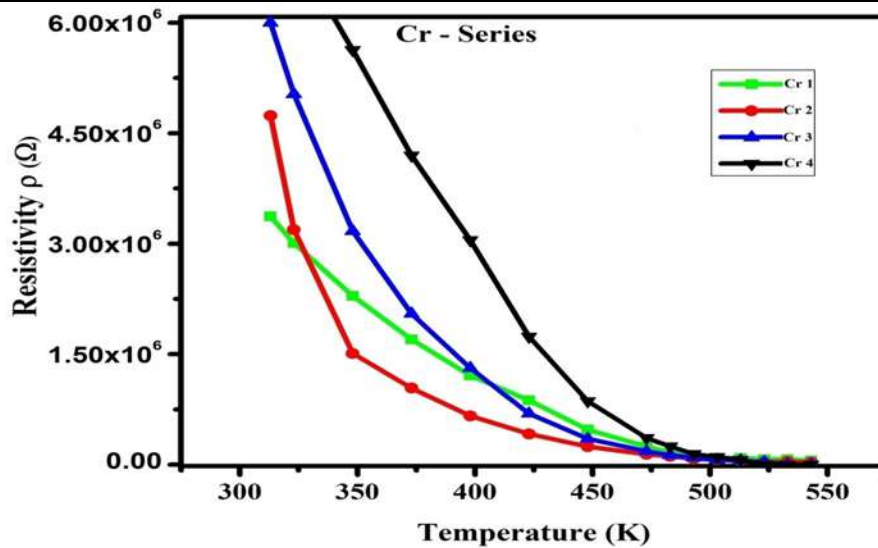


Figure 2. D.C electrical resistivity Verses Temperature

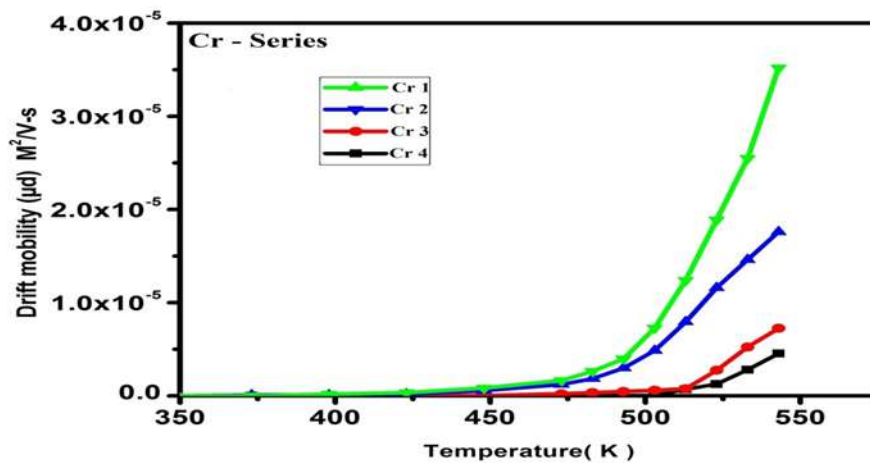


Figure 3. Drift mobility of $Mg_{(1+x)}Zr_x(CrFe)_{1-x}O_4$ ($x = 0.2, 0.4, 0.6, 0.8$) against Temperature
 Table 2. Electrical properties

3.3. Effect of Zr- Mg composition on D.C. Resistivity

With the increase in concentration of Zr-Mg ferrite system it is observed that the DC electrical resistivity at room temperature i.e. 300K was found to increase as shown in table 2. The variations in resistivity with composition can be explained by hopping mechanism [11]. The electronic conduction in the synthesized ferrites is mainly due to hopping of electrons between the ions of the same element with different oxidation state (Fe²⁺ and Fe³⁺ ions) and distributed randomly over equivalent lattice sites [12]. The hopping of electrons mainly depends upon two factors such as separation between the ions and activation energy of the prepared sample. We know that Zr⁴⁺ has strong preference for tetrahedral (A) site similarly Cr³⁺ ions have strongly occupied in



octahedral (B) site, and Mg^{2+} partially distributed over both A and B site. Hence, with decreasing Cr and Fe content means Zr and Mg increases therefore Fe^{3+} ions are partially replaced by Mg^{2+} ions at B-sites. As zirconium has the larger ionic radii so it helps to separate the distance between A and B site larger as the substitution of Zr ions enhanced. Therefore it consequently decreases the shifting of Fe ions from A site to B site and hence the hopping between the Fe^{2+} and Fe^{3+} decrease and this causes the higher resistive of sample as shown in table 2.

IV. CONCLUSIONS

With sol – gel auto combustion route, Zr – Mg substituted Chromium spinel ferrite nano particles have been effectively and successfully synthesized. XRD data reveals that the phase presence of spinel ferrite for all the samples and lattice parameter was found to be increases for higher concentration of zirconium. $Mg_{(1+x)}Zr_x(CrFe)_{1-x}O_4$ ($x = 0.2, 0.4, 0.6, 0.8$) nano spinel ferrite samples show semiconducting behavior with DC electrical resistivity and decreasing with increasing the temperature. At room temperature resistivity for a ferrite sample is very high and decreases with an increase in temperature, resistivity of sample varies from $3.37 \times 10^6 \text{ M}\Omega\text{-cm}$ to $7.71 \times 10^6 \text{ M}\Omega\text{-cm}$. The activation energy for all the samples is found to be different for ferrimagnetic and paramagnetic region. The activation energy in ferrimagnetic region is observed to be less than that in paramagnetic region.

V. ACKNOWLEDGEMENT:

One of the Author N.N. Sarkar acknowledges to the Department of Physics of Dr. Ambedkar College, Deeksha Bhoomi, Nagpur for extending their support to carryout research work

VI. REFERENCE

- [1] N. N. Sarkar, K. Rewatkar, N. S. Meshram, and V. Nanoti, "Structural and magnetic studies of $(Ni_{0.5}M_{0.5}Fe_2O_4)$ where $M = Zn, Cu$," *Ferroelectrics*, vol. 519, pp. 209–212, Oct. 2017.
- [2] N. N. Sarkar, K. G. Rewatkar, V. M. Nanoti, P. S. Hedao, and M.N.Giriya, "Cation Distribution of $Zn_{0.5}Me_{0.5}Fe_2O_4$ ($Me = Co, Ni$ And Cu) on the Basis of Rietveld Refinement and Magnetization Measurement," *Material Science Research India*, vol. 14, no. 2, Dec. 2017.
- [3] A. D. Deshpande, K. G. Rewatkar, and V. M. Nanoti, "Study of Morphology and Magnetic Properties of Nanosized Particles of Zirconium – Cobalt Substituted Calcium Hexaferrites," *Materials Today: Proceedings*, vol. 4, no. 11, pp. 12174–12179, 2017.
- [4] K. Jalaiah, K. Chandra mouli, P. S. V. Subba Rao, and B. Sreedhar, "Structural and dielectric properties of Zr and Cu co-substituted $Ni_{0.5}Zn_{0.5}Fe_2O_4$," *Journal of Magnetism and Magnetic Materials*, vol. 432, no. Supplement C, pp. 418–424, Jun. 2017.
- [5] Christo Ananth, "A Novel NN Output Feedback Control Law For Quad Rotor UAV", *International Journal of Advanced Research in Innovative Discoveries in Engineering and Applications [IJARIDEA]*, Volume 2, Issue 1, February 2017, pp: 18-26.
- [6] M. El - Shabasy, "DC electrical properties of Zn Ni ferrites," *J. Magn. Magn. Mater.*, vol. 172, no. 1, pp. 188–192, Aug. 1997.
- [7] H. S. Ahamad, N. S. Meshram, S. B. Bankar, S. J. Dhoble, and K. G. Rewatkar, "Structural properties of $Cu_xNi_{1-x}Fe_2O_4$ nano ferrites prepared by urea-gel microwave auto combustion method," *Ferroelectrics*, vol. 516, no. 1, pp. 67–73, 2017.
- [8] K. Shetty *et al.*, "Designing $MgFe_2O_4$ decorated on green mediated reduced graphene oxide sheets showing photocatalytic performance and luminescence property," *Physica B: Condensed Matter*, vol. 507, pp. 67–75, 2017.
- [9] M. A. Elkestawy, S. Abdel kader, and M. A. Amer, "AC conductivity and dielectric properties of Ti-doped $CoCr_{1.2}Fe_{0.8}O_4$ spinel ferrite," *Physica B: Condensed Matter*, vol. 405, no. 2, pp. 619–624, 2010.
- [10] L. Li, X. Tu, L. Peng, and X. Zhu, "Structure and static magnetic properties of Zr-substituted NiZn ferrite thin films synthesized by sol–gel process," *Journal of Alloys and Compounds*, vol. 545, no. Supplement C, pp. 67–69, Dec. 2012.
- [11] S. Nazir *et al.*, "Structural, spectral, dielectric and photocatalytic studies of Zr-Ni doped $MnFe_2O_4$ co-precipitated nanoparticles," *Ceramics International*, vol. 42, no. 12, pp. 13459–13463, Sep. 2016.
- [12] Y. B. Kannan, R. Saravanan, N. Srinivasan, and I. Ismail, "Sintering effect on structural, magnetic and optical properties of $Ni_{0.5}Zn_{0.5}Fe_2O_4$ ferrite nano particles," *Journal of Magnetism and Magnetic Materials*, vol. 423, no. Supplement C, pp. 217–225, Feb. 2017.